PROCEEDINGS OF SCIENCE

Monitoring the inter-calibration of the HEAT and Coihueco fluorescence telescopes of the Pierre Auger Observatory with measurements of the brightness of the night sky

A. Segreto[a,b,*] **on behalf of the Pierre Auger**[c] **Collaboration**

[a] *INAF-IASF, Via Ugo La Malfa 153, Palermo, Italy*
[b] *INFN Sezione di Catania, Via S. Sofia, 64, Catania, Italy*
[c] *Observatorio Pierre Auger, Av. San Martín Norte 304, 5613 Malargüe, Argentina*
Full author list: https://www.auger.org/archive/authors_icrc_2023.html

E-mail: spokespersons@auger.org

The High Elevation Auger Telescopes (HEAT) has increased the Field of View (FoV) of the Fluorescence Detector (FD) at the Coihueco site of the Pierre Auger Observatory and allowed the extension of the energy threshold for the measurements of energies and $X_{\max}$ of Extensive Air Showers (EAS) down to $\approx 10^{17.2}$ eV. By temporarily orienting HEAT in the downward position, it acquires data in the same FoV as the other Coihueco telescopes, thus providing the opportunity to intercalibrate the detectors by multiple observations of the same EAS.
To further control systematic uncertainties in $X_{\max}$ and energy measurements, in this contribution we present an innovative method that takes advantage of the Night Sky Brightness (NSB) continuously measured with the FD data acquisition system for monitoring a possible evolution in time of the initial HEAT and Coihueco inter-calibration.
While the brightness of the night sky evolves unpredictably and is highly dependent on local weather conditions, we expect to obtain consistent measurements from telescopes located at the same site and observing the same direction of the sky.
In this work, we describe the method used to compare the NSB measured by the neighboring HEAT and Coihueco telescopes to monitor the stability of their relative calibration over time. This method allows us to study further the systematics in the inter-calibration of the FD telescopes.

The 38th International Cosmic Ray Conference (ICRC2023)
26 July – 3 August, 2023
Nagoya, Japan

*Speaker

PoS(ICRC2023)276

1. Introduction

The Fluorescence Detector (FD) of the Pierre Auger Observatory comprises 27 telescopes, with $30^\circ \times 28^\circ$ FoV, each one having a spherical surface camera consisting of an array of 20 rows by 22 columns of hexagonal photo-multiplier tubes (PMTs) [1].

With the installation of the three fluorescence High Elevation Auger Telescopes (HEAT) at the Coihueco site [2], the FoV of the HEAT/Coihueco system (HECo) increased significantly with respect to the Coihueco FoV alone. This upgrade allows us to see fluorescence light emitted from showers occurring in the upper atmosphere, produced by lower energy cosmic rays, where otherwise the shower maximum would be above the FoV. This was important to extend the $X_{\rm max}$ analysis to lower energies, to be able to calibrate the 750 m surface detector, and to advance the study of the mass composition of lower-energy cosmic rays.

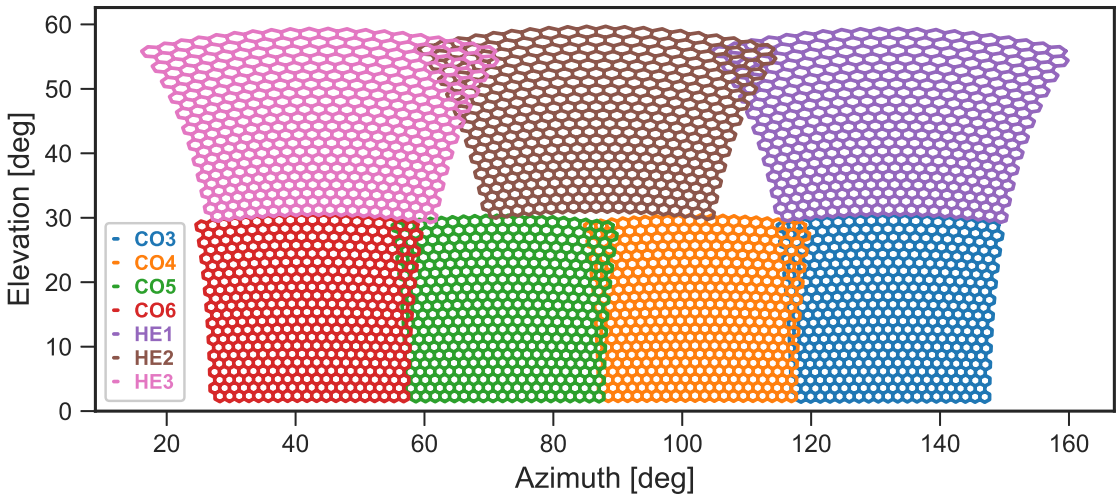

Figure 1: The FoV of the 3 HEAT telescopes (when it is in an upward position) and of the 4 (out of 6) Coihueco telescopes that observe the sky in the same azimuthal range observed by HEAT.

The HEAT telescopes are mounted in separate containers which can be tilted by 30° and allow the telescopes to observe the sky up to $\approx 60^\circ$. In Fig. 1, the total FoV observed by the 3 HEAT telescopes and by 4 (out of 6) Coihueco telescopes, which are observing the sky in the same azimuthal range as observed by HEAT, is shown.

Absolute end-to-end calibration of all FD telescopes is performed by mounting a large-diameter uniform light source [3] on each telescope and illuminating the entire aperture with a known photon flux. This calibration is performed only a few times, while a relative calibration is done each data-taking night to track changes in PMT gains from the absolute reference calibration.

In the normal operation mode, the HEAT telescopes are oriented in the upwards position; however, occasionally, the telescopes are shifted to the downward position to acquire data in the same FoV as the Coihueco telescopes. This allows us to inter-calibrate the telescopes by multiple observations of the same EAS.

In an attempt to further monitor the possible evolution of the initial inter-calibration of the HEAT and Coihueco telescopes during the normal observation period, with HEAT in the upward

position, in this contribution, we present a novel method based on the analysis of the NSB observed continuously by the FD telescopes. We developed two algorithms to take advantage of the fact that while the brightness of the night sky evolves unpredictably and depends strongly on local weather conditions, we expect to obtain consistent measurements from telescopes located at the same site and which are observing the same region of the sky.

2. The NSB as inter-calibration tool

The NSB is generated by various independent sources such as stars and planets, moonlight, twilight, airglow, and zodiacal light, and its intensity is strongly influenced by local atmospheric conditions, such as the presence of clouds and the amount of aerosol scattering in the atmosphere.

The NSB is therefore characterized by unpredictable temporal evolution, both during the night and from night to night, so it cannot be used as a reference illumination level for the telescope calibration. However, if we consider two telescopes located at the same site and observing the sky in the same region, we expect to obtain the same flux measurements, apart from a scaling factor depending on their relative calibration.

In the case of FD telescopes, the NSB measurements are obtained starting from the PMT's baseline variance measurements.

2.1 The baseline variance

The anode current of the PMTs in the FD camera is proportional to the light present in the FoV of the pixel, however, since the electronic readout of the PMTs is AC-coupled, direct measurement of the continuous or slow varying component of the anode current, such as that induced by the NSB cannot be performed.

However, an indirect measurement of the background light is possible by exploiting the high-frequency fluctuations of the anode current induced by the Poissonian nature of the light. Since the intensity of these fluctuations is proportional to the count rate of photons reaching the PMT, the variance of the PMT baseline signal allows us to derive the NSB intensity.

The variance is calculated continuously using $N = 2^{16}$ ADC samples provided by the digitizer and the result is stored in the FD background files every 30 s, which is sufficient to monitor the time evolution of the NSB.

The relative statistical accuracy of each FD variance measurement is $\sqrt{2/N} \approx 0.55\%$. To illustrate this accuracy, in Fig. 2 we show the time evolution of the baseline variance acquired from two pixels placed in separate telescopes, but observing the same region of the sky. In the left panel, we compare two pixels with overlapping FoVs in CO4 and CO5, while in the right panel, we select two pixels in HE1 and HE2. Apart from a scaling factor, which depends on differences in the gain and noise characteristics of the PMTs, the similarity between the curves shows as the FD variance effectively tracks the NSB including fluctuations smaller than 1%.

In the selected night, during the first few hours, the variance is characterized by rapid irregular fluctuations due to the presence of clouds, while in the second part of the night, the sky becomes clear and the observed variations are due to the transit of several faint stars in the FoV of the pixels.

The level of accuracy of the baseline variance for monitoring the NSB was also verified using a small telescope working in single photon counting mode, placed on top of one FD telescope

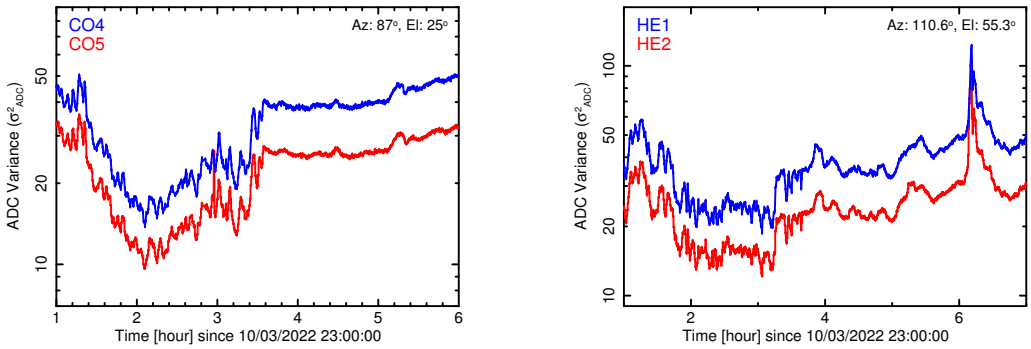

Figure 2: Examples of nighttime evolution of the baseline variance, obtained from pairs of pixels observing the same region of the sky from different telescopes (CO4, CO5 on the left panel, HE1, HE2 on the right panel). Apart from a scaling factor, which depends on differences in the gain and noise characteristics of the PMTs, the light curves show identical fluctuations at the sub-percent level both under cloudy sky conditions, at the beginning of the night, and under clear sky conditions during the second part of the night when the transit of several stars (of 5^{th} magnitude) in the FoV of the pixels is observed.

building [4]. Comparison of the sky background flux measured by the two different methods (baseline variance vs. single photon counting) in the same sky direction showed to be proportional in a very wide range of values.

The variance calculation was initially implemented as a safety tool to monitor the presence of excessive light in the FD telescopes FoV (e.g. to limit the exposure to moonlight) and for determining the pointing of telescopes through signals induced by the transit of bright stars [5]. In the following sections, we show how variance data can be also used as a tool to monitor the inter-calibration among FD telescopes.

2.2 From baseline variance to NSB physical unit

For telescope inter-calibration analysis, we need to convert the baseline variance of the PMT ADC traces ($\sigma^2_{\rm ADC}$) measured under night sky illumination to brightness physical units (e.g. photons $\mathrm{m}^{-2}\,\mathrm{sr}^{-1}\,\mu\mathrm{s}^{-1}$). The first step is to subtract the contribution due to electronic noise and PMTs dark current from the variance, by using the acquisitions done each night before starting the data taking with the PMTs in dark conditions.

The result is directly proportional to the NSB flux in the pixel FoV. The scaling factor depends on the end-to-end optical efficiency of the telescope, the square of the PMT gain, the bandwidth of the electronic amplification system, and the noise factor of the PMT. To convert the variance into physical NSB units, besides the absolute pixel calibration constants, we need a second scaling factor that takes into account the PMT noise characteristics. This factor can be directly measured from the analysis of the calibration pulses generated by UV LED of the relative calibration system [4].

3. Using the NSB for the HEAT and Coihueco inter-calibration

In the case of HEAT and Coihueco telescopes, since their FoVs in the normal acquisition configuration do not overlap, the direct comparison of NSB in precisely (within a few arcmins)

directions of the sky is not possible.

A possible alternative, which has first been implemented, is the direct comparison of the average value of the NSB measured by pixels selected in the boundary region of the two telescopes (e.g. within 5° from the lower boundary of HEAT FoV and the upper edge of Coihueco FoV). In this method, it is assumed that the NSB variations with elevation caused by atmospheric extinction are negligible. In addition, pixels that are affected by bright point sources are removed before calculating the average NSB, as the result could be significantly different in sky directions differing by just a few degrees.

To take also into account NSB variation with elevation, we use a 2-D analytical function to model the diffuse component of NSB over the entire FoV of the telescopes, excluding the contribution of bright point sources and local fluctuations due to clouds, and then calculate the ratio of the two analytical models in appropriate sky directions near the FoV of the two telescopes. Since the NSB analytical models depend on the average collective behavior of all camera pixels, their ratio is not sensitive to any problem that may affect individual pixels thus it is representative of the average inter-calibration status of the two telescopes.

We begin the procedure by identifying (using known sky coordinates) the camera pixels that are expected to be illuminated by bright stars or planets then fit a low-order 2D polynomial to the sky image formed by the remaining pixels. If outliers are found in the residual image (e.g., due to pixel calibration problems or the presence of clouds), we exclude them and repeat the fitting procedure until no new outliers are found.

The best-fit parameters (i.e. the coefficients of the polynomial function) and the RMS of the residual image are then stored, and the procedure is repeated for all variance frames acquired by the FD telescope during the selected night.

The result of this fitting procedure allows reconstruction of the temporal evolution of the NSB diffuse component in any azimuthal (A_z) and elevation (E_l) direction within or close to the edge of the telescope FoV. Denoting with Az_0, El_0 the pointing direction of the FD telescope axis, the NSB diffuse component is reconstructed by the formula

$$\Phi(Az, El, t_i) = a(t_i) + b(t_i) \cdot \Delta Az + c(t_i) \cdot \Delta El + d(t_i) \cdot (\Delta Az)^2 + e(t_i) \cdot (\Delta El)^2 + \dots$$

where t_i is the acquisition time of the variance frame and $\Delta Az = Az - Az_0$ and $\Delta El = El - El_0$, are the offsets of sky coordinates with respect to the telescope axis.

The analysis of the best-fit coefficients shows that a 3^{rd} order polynomial model is perfectly adequate to describe the NSB elevation dependence while introducing higher order terms does not improve the fit. This simple analytical modeling then allows us to eliminate any possible bias in the NSB ratio due to atmospheric extinction besides allowing us to identify efficiently cloudy nights that are then removed from the analysis. This better rejection of bad periods makes the results more stable.

In Fig. 3 we show an example of NSB vertical profiles from the HE1 and CO3 analytical models calculated at two different times on the same night. The evident discontinuity in the two NSBs measured by the two telescopes corresponds to a difference in relative calibration. It also shows that by rescaling the profiles (in this case HE1, red line), the discontinuity between the telescopes is eliminated and a smooth NSB profile as a function of elevation is obtained, as expected from

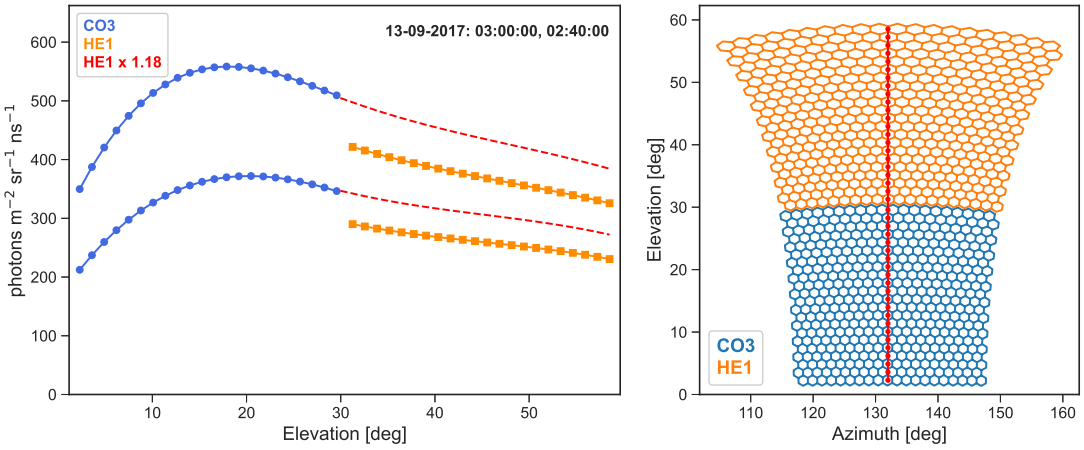

Figure 3: Vertical profiles obtained from the analytical model of the diffuse NSB for CO1 (blue) and HE1 (orange) calculated along a vertical line through the two telescopes at two moments of the same night. The evident discontinuity between the two data sets can be restored by scaling properly the profiles; for example, by scaling the HE1 data by 1.18 (red line).

the air-glow emission. This confirms that the selected analytical model effectively eliminates any biasing effect due to the NSB vertical gradient

3.1 Computation of the "NSB ratio"

Once obtained analytical models of the diffuse NSB for two FD telescopes with adjacent FOVs, we select a sky region close to the FoV edge of both telescopes and calculate their relative difference as:

$$\Delta\Phi(Az, El, t) = \frac{\Phi_{tel2}(Az, El, t) - \Phi_{tel1}(Az, El, t)}{\Phi_{tel2}(Az, El, t) + \Phi_{tel1}(Az, El, t)}$$

where Φ_{tel1} and Φ_{tel2} are the analytical NSB models for the two selected telescopes.

For example, in the upper panel of Fig. 4a we show the temporal evolution of the diffuse NSB relative to Coihueco Bay 3 (CO3) and HEAT Bay 1 (HE1) calculated in the sky direction $Az = 132°$, $El = 30.4°$ and, in the lower panel, their relative difference. In this case, the sky brightness measured from HE1 is systematically lower throughout the night than the simultaneous measurement obtained from CO3.

A robust fit of the relative difference is then performed, to exclude any period in which the temporal evolution between the two NSB curves is not consistent, such as it may occur in the presence of clouds or extended star clusters, like the Galactic plane, which cannot be modeled by a low-order polynomial or excluded completely from the NSB fit. If an extended period (at least a few hours) is obtained, in which the relative difference is almost constant, the average "NSB ratio" (NSB_R) for the selected night is calculated by

$$NSB_R(Az, El) = \frac{1 + < \Delta\Phi(Az, El, t) >}{1 - < \Delta\Phi(Az, El, t) >}$$

where $< \Delta\Phi(Az, El, t) >$ is the robust average of the NSB relative difference through the night.

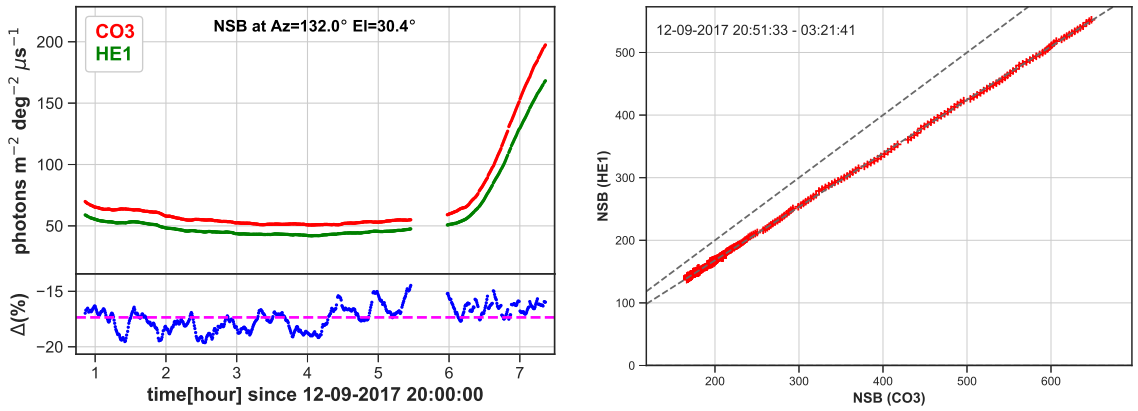

(a) **(b)**

Figure 4: In the left figure, the upper panel shows the comparison of the nighttime evolution of the analytical model of NSB for two adjacent telescopes, calculated in the same sky direction, while the lower panel shows the relative difference. The right figure shows the linear correlation existing between the two NSB measurements.

In Fig. 4b right panel, we show for the same night, the correlation existing between the two models, that demonstrate a linear correlation over a large range of brightness values, although with a slope significantly lower than unity.

4. NSB ratio long-term evolution

Neither telescope can be considered a priori as a reference, however, a comparison of the NSB_R from multiple telescopes and their correlation with hardware maintenance interventions can provide rigorous indications of which telescope needs to be corrected.

In Fig. 5 we show an example of the long-term evolution of the NSB_R obtained by comparing the NSB seen by the HE2 telescope with the NSB measured by two telescopes having an adjacent FoV, CO4 (Fig. 5a) and CO5 (Fig. 5b). Several discontinuities are observed in the two profiles, most of which are related to hardware maintenance operations on the telescopes. In particular, the significant discontinuity observed in November 2016 in the HE1/CO5 NSB ratio corresponds to the cleaning of the CO5 mirrors which led to a significant increase in reflectivity. The temporary drop in both the HE2/CO4 and HE2/CO5 NSB ratio during the year 2014, is most likely due to the incomplete opening of the safety curtains that blocked a fraction of the HE2 telescope aperture during that period.

5. Conclusions

We presented a novel method to monitor the relative calibration of FD telescopes exploiting the brightness of the night sky which is measured continuously by the FD data acquisition system. The method allowed us to detect discontinuities in the inter-calibration between the HEAT and Coihueco telescopes caused by maintenance operations or mechanical problems with the fail-safe curtain, leading to the calculation of cross-calibration factors. It is planned to extend this

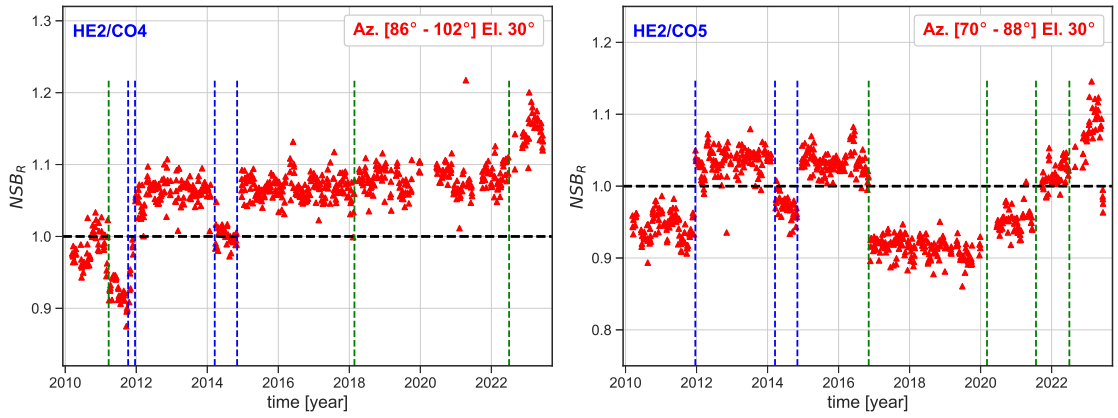

(a) **(b)**

Figure 5: Long-term evolution of the NSB ratio obtained by comparing HE2 with the adjacent bays CO4 (left panel) and CO5 (right panel). The discontinuities observed correspond to hardware maintenance operations on the telescopes, such as cleaning the mirrors or changing the calibration unit.

analysis to all other FD telescopes to integrate the new end-to-end absolute calibration system, the XY-Scanner [6], with which a preliminary comparison shows good agreement.

The method shown is quite general and can also be applied to any other kind of telescope, such as Cherenkov telescopes where, because of the large aperture, artificial end-to-end calibration sources cannot be used frequently.

References

[1] J. Abraham, P. Abreu, M. Aglietta, C. Aguirre, E. Ahn, D. Allard et al., *The fluorescence detector of the Pierre Auger Observatory*, *Nuclear Instruments and Methods in Physics Research Section A: Accelerators, Spectrometers, Detectors and Associated Equipment* **620** (2010) 227.

[2] Pierre Auger collaboration, *The Pierre Auger Cosmic Ray Observatory*, *Nucl. Instrum. Meth. A* **798** (2015) 172 [1502.01323].

[3] J.T. Brack, R. Meyhandan, G.J. Hofman and J. Matthews, *Absolute photometric calibration of large aperture optical systems*, *Astroparticle Physics* **20** (2004) 653.

[4] A. Segreto, *Night Sky Background measurements by the Pierre Auger Fluorescence Detectors and comparison with simultaneous data from the UVscope instrument.*, in *International Cosmic Ray Conference*, vol. 3 of *International Cosmic Ray Conference*, p. 129, Jan., 2011, DOI.

[5] C. De Donato, M. Prouza, F. Sanchez, M. Santander, D. Camin, B. Garcia et al., *Using stars to determine the absolute pointing of the fluorescence detector telescopes of the Pierre Auger Observatory*, *Astroparticle Physics* **28** (2007) 216.

[6] C.M. Schäfer and The Pierre Auger Collaboration, *A Novel Tool for the Absolute End-to-End Calibration of Fluorescence Telescopes – The XY-Scanner*, in *these proceedings*.

The Pierre Auger Collaboration

A. Abdul Halim[13], P. Abreu[72], M. Aglietta[54,52], I. Allekotte[1], K. Almeida Cheminant[70], A. Almela[7,12], R. Aloisio[45,46], J. Alvarez-Muñiz[79], J. Ammerman Yebra[79], G.A. Anastasi[54,52], L. Anchordoqui[86], B. Andrada[7], S. Andringa[72], C. Aramo[50], P.R. Araújo Ferreira[42], E. Arnone[63,52], J. C. Arteaga Velázquez[67], H. Asorey[7], P. Assis[72], G. Avila[11], E. Avocone[57,46], A.M. Badescu[75], A. Bakalova[32], A. Balaceanu[73], F. Barbato[45,46], A. Bartz Mocellin[85], J.A. Bellido[13,69], C. Berat[36], M.E. Bertaina[63,52], G. Bhatta[70], M. Bianciotto[63,52], P.L. Biermann[h], V. Binet[5], K. Bismark[39,7], T. Bister[80,81], J. Biteau[37], J. Blazek[32], C. Bleve[36], J. Blümer[41], M. Boháčová[32], D. Boncioli[57,46], C. Bonifazi[8,26], L. Bonneau Arbeletche[21], N. Borodai[70], J. Brack[j], P.G. Brichetto Orchera[7], F.L. Briechle[42], A. Bueno[78], S. Buitink[15], M. Buscemi[47,61], M. Büsken[39,7], A. Bwembya[80,81], K.S. Caballero-Mora[66], S. Cabana-Freire[79], L. Caccianiga[59,49], I. Caracas[38], R. Caruso[58,47], A. Castellina[54,52], F. Catalani[18], G. Cataldi[48], L. Cazon[79], M. Cerda[10], A. Cermenati[45,46], J.A. Chinellato[21], J. Chudoba[32], L. Chytka[33], R.W. Clay[13], A.C. Cobos Cerutti[6], R. Colalillo[60,50], A. Coleman[90], M.R. Coluccia[48], R. Conceição[72], A. Condorelli[37], G. Consolati[49,55], M. Conte[56,48], F. Convenga[41], D. Correia dos Santos[28], P.J. Costa[72], C.E. Covault[84], M. Cristinziani[44], C.S. Cruz Sanchez[3], S. Dasso[4,2], K. Daumiller[41], B.R. Dawson[13], R.M. de Almeida[28], J. de Jesús[7,41], S.J. de Jong[80,81], J.R.T. de Mello Neto[26,27], I. De Mitri[45,46], J. de Oliveira[17], D. de Oliveira Franco[21], F. de Palma[56,48], V. de Souza[19], E. De Vito[56,48], A. Del Popolo[58,47], O. Deligny[34], N. Denner[32], L. Deval[41,7], A. di Matteo[52], M. Dobre[73], C. Dobrigkeit[21], J.C. D'Olivo[68], L.M. Domingues Mendes[72], J.C. dos Anjos, R.C. dos Anjos[25], J. Ebr[32], F. Ellwanger[41], M. Emam[80,81], R. Engel[39,41], I. Epicoco[56,48], M. Erdmann[42], A. Etchegoyen[7,12], C. Evoli[45,46], H. Falcke[80,82,81], J. Farmer[89], G. Farrar[88], A.C. Fauth[21], N. Fazzini[e], F. Feldbusch[40], F. Fenu[41,d], A. Fernandes[72], B. Fick[87], J.M. Figueira[7], A. Filipčič[77,76], T. Fitoussi[41], B. Flaggs[90], T. Fodran[80], T. Fujii[89,f], A. Fuster[7,12], C. Galea[80], C. Galelli[59,49], B. García[6], C. Gaudu[38], H. Gemmeke[40], F. Gesualdi[7,41], A. Gherghel-Lascu[73], P.L. Ghia[34], U. Giaccari[48], M. Giammarchi[49], J. Glombitza[42,g], F. Gobbi[10], F. Gollan[7], G. Golup[1], M. Gómez Berisso[1], P.F. Gómez Vitale[11], J.P. Gongora[11], J.M. González[1], N. González[7], I. Goos[1], D. Góra[70], A. Gorgi[54,52], M. Gottowik[79], T.D. Grubb[13], F. Guarino[60,50], G.P. Guedes[22], E. Guido[44], S. Hahn[39], P. Hamal[32], M.R. Hampel[7], P. Hansen[3], D. Harari[1], V.M. Harvey[13], A. Haungs[41], T. Hebbeker[42], C. Hojvat[e], J.R. Hörandel[80,81], P. Horvath[33], M. Hrabovský[33], T. Huege[41,15], A. Insolia[58,47], P.G. Isar[74], P. Janecek[32], J.A. Johnsen[85], J. Jurysek[32], A. Kääpä[38], K.H. Kampert[38], B. Keilhauer[41], A. Khakurdikar[80], V.V. Kizakke Covilakam[7,41], H.O. Klages[41], M. Kleifges[40], F. Knapp[39], N. Kunka[40], B.L. Lago[16], N. Langner[42], M.A. Leigui de Oliveira[24], Y Lema-Capeans[79], V. Lenok[39], A. Letessier-Selvon[35], I. Lhenry-Yvon[34], D. Lo Presti[58,47], L. Lopes[72], L. Lu[91], Q. Luce[39], J.P. Lundquist[76], A. Machado Payeras[21], M. Majercakova[32], D. Mandat[32], B.C. Manning[13], P. Mantsch[e], S. Marafico[34], F.M. Mariani[59,49], A.G. Mariazzi[3], I.C. Mariş[14], G. Marsella[61,47], D. Martello[56,48], S. Martinelli[41,7], O. Martínez Bravo[64], M.A. Martins[79], M. Mastrodicasa[57,46], H.J. Mathes[41], J. Matthews[a], G. Matthiae[62,51], E. Mayotte[85,38], S. Mayotte[85], P.O. Mazur[e], G. Medina-Tanco[68], J. Meinert[38], D. Melo[7], A. Menshikov[40], C. Merx[41], S. Michal[33], M.I. Micheletti[5], L. Miramonti[59,49], S. Mollerach[1], F. Montanet[36], L. Morejon[38], C. Morello[54,52], A.L. Müller[32], K. Mulrey[80,81], R. Mussa[52], M. Muzio[88], W.M. Namasaka[38], S. Negi[32], L. Nellen[68], K. Nguyen[87], G. Nicora[9], M. Niculescu-Oglinzanu[73], M. Niechciol[44], D. Nitz[87], D. Nosek[31], V. Novotny[31], L. Nožka[33], A Nucita[56,48], L.A. Núñez[30], C. Oliveira[19], M. Palatka[32], J. Pallotta[9], S. Panja[32], G. Parente[79], T. Paulsen[38], J. Pawlowsky[38], M. Pech[32], J. Pękala[70], R. Pelayo[65], L.A.S. Pereira[23], E.E. Pereira Martins[39,7], J. Perez Armand[20], C. Pérez Bertolli[7,41], L. Perrone[56,48], S. Petrera[45,46], C. Petrucci[57,46], T. Pierog[41], M. Pimenta[72], M. Platino[7], B. Pont[80], M. Pothast[81,80], M. Pourmohammad Shahvar[61,47], P. Privitera[89], M. Prouza[32], A. Puyleart[87], S. Querchfeld[38], J. Rautenberg[38], D. Ravignani[7], M. Reininghaus[39], J. Ridky[32], F. Riehn[79], M. Risse[44], V. Rizi[57,46], W. Rodrigues de Carvalho[80], E. Rodriguez[7,41], J. Rodriguez Rojo[11], M.J. Roncoroni[7], S. Rossoni[43], M. Roth[41], E. Roulet[1], A.C. Rovero[4], P. Ruehl[44], A. Saftoiu[73], M. Saharan[80], F. Salamida[57,46], H. Salazar[64], G. Salina[51], J.D. Sanabria Gomez[30], F. Sánchez[7], E.M. Santos[20], E. Santos[32],

F. Sarazin[85], R. Sarmento[72], R. Sato[11], P. Savina[91], C.M. Schäfer[41], V. Scherini[56,48], H. Schieler[41], M. Schimassek[34], M. Schimp[38], F. Schlüter[41], D. Schmidt[39], O. Scholten[15,i], H. Schoorlemmer[80,81], P. Schovánek[32], F.G. Schröder[90,41], J. Schulte[42], T. Schulz[41], S.J. Sciutto[3], M. Scornavacche[7,41], A. Segreto[53,47], S. Sehgal[38], S.U. Shivashankara[76], G. Sigl[43], G. Silli[7], O. Sima[73,b], F. Simon[40], R. Smau[73], R. Šmída[89], P. Sommers[k], J.F. Soriano[86], R. Squartini[10], M. Stadelmaier[32], D. Stanca[73], S. Stanič[76], J. Stasielak[70], P. Stassi[36], S. Strähnz[39], M. Straub[42], M. Suárez-Durán[14], T. Suomijärvi[37], A.D. Supanitsky[7], Z. Svozilikova[32], Z. Szadkowski[71], A. Tapia[29], C. Taricco[63,52], C. Timmermans[81,80], O. Tkachenko[41], P. Tobiska[32], C.J. Todero Peixoto[18], B. Tomé[72], Z. Torrès[36], A. Travaini[10], P. Travnicek[32], C. Trimarelli[57,46], M. Tueros[3], M. Unger[41], L. Vaclavek[33], M. Vacula[33], J.F. Valdés Galicia[68], L. Valore[60,50], E. Varela[64], A. Vásquez-Ramírez[30], D. Veberič[41], C. Ventura[27], I.D. Vergara Quispe[3], V. Verzi[51], J. Vicha[32], J. Vink[83], J. Vlastimil[32], S. Vorobiov[76], C. Watanabe[26], A.A. Watson[c], A. Weindl[41], L. Wiencke[85], H. Wilczyński[70], D. Wittkowski[38], B. Wundheiler[7], B. Yue[38], A. Yushkov[32], O. Zapparrata[14], E. Zas[79], D. Zavrtanik[76,77], M. Zavrtanik[77,76]

———— • ————

[1] Centro Atómico Bariloche and Instituto Balseiro (CNEA-UNCuyo-CONICET), San Carlos de Bariloche, Argentina
[2] Departamento de Física and Departamento de Ciencias de la Atmósfera y los Océanos, FCEyN, Universidad de Buenos Aires and CONICET, Buenos Aires, Argentina
[3] IFLP, Universidad Nacional de La Plata and CONICET, La Plata, Argentina
[4] Instituto de Astronomía y Física del Espacio (IAFE, CONICET-UBA), Buenos Aires, Argentina
[5] Instituto de Física de Rosario (IFIR) – CONICET/U.N.R. and Facultad de Ciencias Bioquímicas y Farmacéuticas U.N.R., Rosario, Argentina
[6] Instituto de Tecnologías en Detección y Astropartículas (CNEA, CONICET, UNSAM), and Universidad Tecnológica Nacional – Facultad Regional Mendoza (CONICET/CNEA), Mendoza, Argentina
[7] Instituto de Tecnologías en Detección y Astropartículas (CNEA, CONICET, UNSAM), Buenos Aires, Argentina
[8] International Center of Advanced Studies and Instituto de Ciencias Físicas, ECyT-UNSAM and CONICET, Campus Miguelete – San Martín, Buenos Aires, Argentina
[9] Laboratorio Atmósfera – Departamento de Investigaciones en Láseres y sus Aplicaciones – UNIDEF (CITEDEF-CONICET), Argentina
[10] Observatorio Pierre Auger, Malargüe, Argentina
[11] Observatorio Pierre Auger and Comisión Nacional de Energía Atómica, Malargüe, Argentina
[12] Universidad Tecnológica Nacional – Facultad Regional Buenos Aires, Buenos Aires, Argentina
[13] University of Adelaide, Adelaide, S.A., Australia
[14] Université Libre de Bruxelles (ULB), Brussels, Belgium
[15] Vrije Universiteit Brussels, Brussels, Belgium
[16] Centro Federal de Educação Tecnológica Celso Suckow da Fonseca, Petropolis, Brazil
[17] Instituto Federal de Educação, Ciência e Tecnologia do Rio de Janeiro (IFRJ), Brazil
[18] Universidade de São Paulo, Escola de Engenharia de Lorena, Lorena, SP, Brazil
[19] Universidade de São Paulo, Instituto de Física de São Carlos, São Carlos, SP, Brazil
[20] Universidade de São Paulo, Instituto de Física, São Paulo, SP, Brazil
[21] Universidade Estadual de Campinas, IFGW, Campinas, SP, Brazil
[22] Universidade Estadual de Feira de Santana, Feira de Santana, Brazil
[23] Universidade Federal de Campina Grande, Centro de Ciencias e Tecnologia, Campina Grande, Brazil
[24] Universidade Federal do ABC, Santo André, SP, Brazil
[25] Universidade Federal do Paraná, Setor Palotina, Palotina, Brazil
[26] Universidade Federal do Rio de Janeiro, Instituto de Física, Rio de Janeiro, RJ, Brazil
[27] Universidade Federal do Rio de Janeiro (UFRJ), Observatório do Valongo, Rio de Janeiro, RJ, Brazil
[28] Universidade Federal Fluminense, EEIMVR, Volta Redonda, RJ, Brazil
[29] Universidad de Medellín, Medellín, Colombia
[30] Universidad Industrial de Santander, Bucaramanga, Colombia

[31] Charles University, Faculty of Mathematics and Physics, Institute of Particle and Nuclear Physics, Prague, Czech Republic
[32] Institute of Physics of the Czech Academy of Sciences, Prague, Czech Republic
[33] Palacky University, Olomouc, Czech Republic
[34] CNRS/IN2P3, IJCLab, Université Paris-Saclay, Orsay, France
[35] Laboratoire de Physique Nucléaire et de Hautes Energies (LPNHE), Sorbonne Université, Université de Paris, CNRS-IN2P3, Paris, France
[36] Univ. Grenoble Alpes, CNRS, Grenoble Institute of Engineering Univ. Grenoble Alpes, LPSC-IN2P3, 38000 Grenoble, France
[37] Université Paris-Saclay, CNRS/IN2P3, IJCLab, Orsay, France
[38] Bergische Universität Wuppertal, Department of Physics, Wuppertal, Germany
[39] Karlsruhe Institute of Technology (KIT), Institute for Experimental Particle Physics, Karlsruhe, Germany
[40] Karlsruhe Institute of Technology (KIT), Institut für Prozessdatenverarbeitung und Elektronik, Karlsruhe, Germany
[41] Karlsruhe Institute of Technology (KIT), Institute for Astroparticle Physics, Karlsruhe, Germany
[42] RWTH Aachen University, III. Physikalisches Institut A, Aachen, Germany
[43] Universität Hamburg, II. Institut für Theoretische Physik, Hamburg, Germany
[44] Universität Siegen, Department Physik – Experimentelle Teilchenphysik, Siegen, Germany
[45] Gran Sasso Science Institute, L'Aquila, Italy
[46] INFN Laboratori Nazionali del Gran Sasso, Assergi (L'Aquila), Italy
[47] INFN, Sezione di Catania, Catania, Italy
[48] INFN, Sezione di Lecce, Lecce, Italy
[49] INFN, Sezione di Milano, Milano, Italy
[50] INFN, Sezione di Napoli, Napoli, Italy
[51] INFN, Sezione di Roma "Tor Vergata", Roma, Italy
[52] INFN, Sezione di Torino, Torino, Italy
[53] Istituto di Astrofisica Spaziale e Fisica Cosmica di Palermo (INAF), Palermo, Italy
[54] Osservatorio Astrofisico di Torino (INAF), Torino, Italy
[55] Politecnico di Milano, Dipartimento di Scienze e Tecnologie Aerospaziali , Milano, Italy
[56] Università del Salento, Dipartimento di Matematica e Fisica "E. De Giorgi", Lecce, Italy
[57] Università dell'Aquila, Dipartimento di Scienze Fisiche e Chimiche, L'Aquila, Italy
[58] Università di Catania, Dipartimento di Fisica e Astronomia "Ettore Majorana", Catania, Italy
[59] Università di Milano, Dipartimento di Fisica, Milano, Italy
[60] Università di Napoli "Federico II", Dipartimento di Fisica "Ettore Pancini", Napoli, Italy
[61] Università di Palermo, Dipartimento di Fisica e Chimica "E. Segrè", Palermo, Italy
[62] Università di Roma "Tor Vergata", Dipartimento di Fisica, Roma, Italy
[63] Università Torino, Dipartimento di Fisica, Torino, Italy
[64] Benemérita Universidad Autónoma de Puebla, Puebla, México
[65] Unidad Profesional Interdisciplinaria en Ingeniería y Tecnologías Avanzadas del Instituto Politécnico Nacional (UPIITA-IPN), México, D.F., México
[66] Universidad Autónoma de Chiapas, Tuxtla Gutiérrez, Chiapas, México
[67] Universidad Michoacana de San Nicolás de Hidalgo, Morelia, Michoacán, México
[68] Universidad Nacional Autónoma de México, México, D.F., México
[69] Universidad Nacional de San Agustin de Arequipa, Facultad de Ciencias Naturales y Formales, Arequipa, Peru
[70] Institute of Nuclear Physics PAN, Krakow, Poland
[71] University of Łódź, Faculty of High-Energy Astrophysics,Łódź, Poland
[72] Laboratório de Instrumentação e Física Experimental de Partículas – LIP and Instituto Superior Técnico – IST, Universidade de Lisboa – UL, Lisboa, Portugal
[73] "Horia Hulubei" National Institute for Physics and Nuclear Engineering, Bucharest-Magurele, Romania
[74] Institute of Space Science, Bucharest-Magurele, Romania
[75] University Politehnica of Bucharest, Bucharest, Romania
[76] Center for Astrophysics and Cosmology (CAC), University of Nova Gorica, Nova Gorica, Slovenia
[77] Experimental Particle Physics Department, J. Stefan Institute, Ljubljana, Slovenia

PoS(ICRC2023)276

[78] Universidad de Granada and C.A.F.P.E., Granada, Spain
[79] Instituto Galego de Física de Altas Enerxías (IGFAE), Universidade de Santiago de Compostela, Santiago de Compostela, Spain
[80] IMAPP, Radboud University Nijmegen, Nijmegen, The Netherlands
[81] Nationaal Instituut voor Kernfysica en Hoge Energie Fysica (NIKHEF), Science Park, Amsterdam, The Netherlands
[82] Stichting Astronomisch Onderzoek in Nederland (ASTRON), Dwingeloo, The Netherlands
[83] Universiteit van Amsterdam, Faculty of Science, Amsterdam, The Netherlands
[84] Case Western Reserve University, Cleveland, OH, USA
[85] Colorado School of Mines, Golden, CO, USA
[86] Department of Physics and Astronomy, Lehman College, City University of New York, Bronx, NY, USA
[87] Michigan Technological University, Houghton, MI, USA
[88] New York University, New York, NY, USA
[89] University of Chicago, Enrico Fermi Institute, Chicago, IL, USA
[90] University of Delaware, Department of Physics and Astronomy, Bartol Research Institute, Newark, DE, USA
[91] University of Wisconsin-Madison, Department of Physics and WIPAC, Madison, WI, USA

—

[a] Louisiana State University, Baton Rouge, LA, USA
[b] also at University of Bucharest, Physics Department, Bucharest, Romania
[c] School of Physics and Astronomy, University of Leeds, Leeds, United Kingdom
[d] now at Agenzia Spaziale Italiana (ASI). Via del Politecnico 00133, Roma, Italy
[e] Fermi National Accelerator Laboratory, Fermilab, Batavia, IL, USA
[f] now at Graduate School of Science, Osaka Metropolitan University, Osaka, Japan
[g] now at ECAP, Erlangen, Germany
[h] Max-Planck-Institut für Radioastronomie, Bonn, Germany
[i] also at Kapteyn Institute, University of Groningen, Groningen, The Netherlands
[j] Colorado State University, Fort Collins, CO, USA
[k] Pennsylvania State University, University Park, PA, USA

Acknowledgments

The successful installation, commissioning, and operation of the Pierre Auger Observatory would not have been possible without the strong commitment and effort from the technical and administrative staff in Malargüe. We are very grateful to the following agencies and organizations for financial support:

Argentina – Comisión Nacional de Energía Atómica; Agencia Nacional de Promoción Científica y Tecnológica (ANPCyT); Consejo Nacional de Investigaciones Científicas y Técnicas (CONICET); Gobierno de la Provincia de Mendoza; Municipalidad de Malargüe; NDM Holdings and Valle Las Leñas; in gratitude for their continuing cooperation over land access; Australia – the Australian Research Council; Belgium – Fonds de la Recherche Scientifique (FNRS); Research Foundation Flanders (FWO); Brazil – Conselho Nacional de Desenvolvimento Científico e Tecnológico (CNPq); Financiadora de Estudos e Projetos (FINEP); Fundação de Amparo à Pesquisa do Estado de Rio de Janeiro (FAPERJ); São Paulo Research Foundation (FAPESP) Grants No. 2019/10151-2, No. 2010/07359-6 and No. 1999/05404-3; Ministério da Ciência, Tecnologia, Inovações e Comunicações (MCTIC); Czech Republic – Grant No. MSMT CR LTT18004, LM2015038, LM2018102, CZ.02.1.01/0.0/0.0/16_013/0001402, CZ.02.1.01/0.0/0.0/18_046/0016010 and CZ.02.1.01/0.0/0.0/17_049/0008422; France – Centre de Calcul IN2P3/CNRS; Centre National de la Recherche Scientifique (CNRS); Conseil Régional Ile-de-France; Département Physique Nucléaire et Corpusculaire (PNC-IN2P3/CNRS); Département Sciences de l'Univers (SDU-INSU/CNRS); Institut Lagrange de Paris (ILP) Grant No. LABEX ANR-10-LABX-63 within the Investissements d'Avenir Programme Grant No. ANR-11-IDEX-0004-02; Germany – Bundesministerium für Bildung und Forschung (BMBF); Deutsche Forschungsgemeinschaft (DFG); Finanzministerium Baden-Württemberg; Helmholtz Alliance for Astroparticle Physics (HAP); Helmholtz-Gemeinschaft Deutscher Forschungszentren (HGF); Ministerium für Kultur und Wissenschaft des Landes Nordrhein-Westfalen; Ministerium für Wissenschaft, Forschung und Kunst des Landes Baden-Württemberg; Italy – Istituto Nazionale di Fisica Nucleare (INFN); Istituto Nazionale di Astrofisica (INAF); Ministero dell'Istruzione, dell'Universitá e della Ricerca (MIUR); CETEMPS Center of Excellence; Ministero degli Affari Esteri (MAE), ICSC Centro Nazionale di Ricerca in High Performance Computing, Big Data and Quantum Computing, funded by European Union NextGenerationEU, reference code CN_00000013;

México – Consejo Nacional de Ciencia y Tecnología (CONACYT) No. 167733; Universidad Nacional Autónoma de México (UNAM); PAPIIT DGAPA-UNAM; The Netherlands – Ministry of Education, Culture and Science; Netherlands Organisation for Scientific Research (NWO); Dutch national e-infrastructure with the support of SURF Cooperative; Poland – Ministry of Education and Science, grants No. DIR/WK/2018/11 and 2022/WK/12; National Science Centre, grants No. 2016/22/M/ST9/00198, 2016/23/B/ST9/01635, 2020/39/B/ST9/01398, and 2022/45/B/ST9/02163; Portugal – Portuguese national funds and FEDER funds within Programa Operacional Factores de Competitividade through Fundação para a Ciência e a Tecnologia (COMPETE); Romania – Ministry of Research, Innovation and Digitization, CNCS-UEFISCDI, contract no. 30N/2023 under Romanian National Core Program LAPLAS VII, grant no. PN 23 21 01 02 and project number PN-III-P1-1.1-TE-2021-0924/TE57/2022, within PNCDI III; Slovenia – Slovenian Research Agency, grants P1-0031, P1-0385, I0-0033, N1-0111; Spain – Ministerio de Economía, Industria y Competitividad (FPA2017-85114-P and PID2019-104676GB-C32), Xunta de Galicia (ED431C 2017/07), Junta de Andalucía (SOMM17/6104/UGR, P18-FR-4314) Feder Funds, RENATA Red Nacional Temática de Astropartículas (FPA2015-68783-REDT) and María de Maeztu Unit of Excellence (MDM-2016-0692); USA – Department of Energy, Contracts No. DE-AC02-07CH11359, No. DE-FR02-04ER41300, No. DE-FG02-99ER41107 and No. DE-SC0011689; National Science Foundation, Grant No. 0450696; The Grainger Foundation; Marie Curie-IRSES/EPLANET; European Particle Physics Latin American Network; and UNESCO.